VARIABLE MOVING BANDWIDTH SSP MINIMIZATION FOR 3D ULTRASOUND MICROSCOPY

CUDEL C.; GREVILLOT M.; MEYER J.J.; SIMONIN L.; JACQUEY S.
LAB.EL/MIPS, Université de Haute Alsace
61, rue Albert Camus
Mulhouse 68093 Cedex
France
Tel. : (33) 3 89 33 76 61
Fax. : (33) 3 89 33 76 05
c.cudel@uha.fr

ABSTRACT

This communication presents a variable Moving Bandwidth Minimization algorithm applied to a 3D ultrasound microscopy system for polymer analysis. The system returns specular echoes representing the porosities to be detected. Due to the material absorption the received echoes have spectral characteristics depending on the porosity depth. Under these conditions, a classical Split Spectrum Processing (SSP) algorithm is not optimal to detect all porosities. Our method is a modified SSP algorithm with a variable analysis bandwidth processing. This method is able to detect coherent echoes having different spectral characteristics. Images obtained are compared with fixed bandwidth SSP and with an optical microscope view of a transparent polymer sample.

1. INTRODUCTION

One of the major drawbacks in ultrasonic nondestructive imaging is due to the background noise from the material microstructure. This noise caused by small stationary random reflectors is time invariant. It can mask the flaw echo even if the target is larger than the high density interfering scatterers. This kind of noise cannot be attenuated by classical correlation or time averaging techniques. To achieve SNR enhancement, a frequency diversity Split Spectrum Processing method has already been used with generally non linear algorithms such as minimization [1]. However SSP absolute minimization is sensitive to the processing parameters and the spectral characteristics of the echoes must be accurately known a priori [2,3]. A modified form of this algorithm, named Moving Bandwidth Minimization (MBM) has been proposed in a previous paper [4]. This method is based on mathematical morphology operators and presents lower parameter sensitivity.

In order to ensure controlled mechanical properties of thermal spray coatings it is important to estimate their porosity rate with a proper non-destructive experimental technique. An acoustic microscope system has been designed for detecting, locating and imaging air bubble inclusions which are inherent in such coatings. This imaging is significant because mechanical properties are governed by the concentration and size of the inclusions [5]. The relations between defect detection efficiency, interrogating ultrasound field, and material structure are not such straight forward as one might expect. Detection of defects involves other factors than the relationship between Ultrasonic (US) field wavelength and flaw size. In a brief survey we can point out ; the ultrasound field characteristics, the inspection path, the physical properties of the material, the measurement technique and the detection algorithm.

Moreover the US field propagating in materials undergoes frequency dependent attenuation due to absorption and scattering [6]. Attenuation is function of the depth of the defect and of the

material texture. If scattering dominates, the centroïd of the echo spectrum is low frequency shifted in proportion as the US field penetrates deeper into the material. To validate our system we used a transparent epoxy polymer phantom allowing to compare our ultrasound picture with the corresponding optical microscope image.

If the classical SSP parameters are maintained fix, this algorithm either misses some flaws or presents an increasing false detection rate.

We show that our method improves detection of defects with variable spectral characteristics and that the modified algorithm outperforms classical minimization methods. Results are presented as a porosity depth image and are compared with the corresponding optical microscope image.

2. THE SSP ABSOLUTE MINIMIZATION AND MBM ALGORITHMS

The quality of ultrasonic images is often plagued by small reflectors surrounding the target. In material evaluation, this parasitic signals are named grain noise. This type of noise results from small, unresolved, randomly distributed scatterers. In such conditions it becomes often difficult to discriminate between the resulting interference pattern and the target signal. The echoes from such stationary scatterers are coherent. The clutter noise can be decorrelated by shifting the transmitted frequency. Indeed a frequency diversity processing affects the large target echoes to a much lesser extent that the small scatterers. The transmitter frequency variation makes the clutter to behave as uncorrelated noise while the target signal remains correlated.

In ultrasonic signal processing the transmitter frequency is maintained constant but the broadband received echo $x(t)$ is split into a ensemble of N overlapping, constant bandwidth, narrowband signals $\chi(t,f_i)$ expressed by

$$\chi(t,f_i) = \text{real}\left[\sum_{i=1}^{N}\left(FT^{-1}(G(f-f_i)X(f))\right)\right]$$

with $G(f-f_i)$ representing a windowing function of center frequency f_i and $X(f)$ the discrete Fourier Transform (FT) of $x(t)$.

Subsequently, after inverse Fourier transformation and amplitude normalization, the resulting signals are combined nonlinearly to obtain the processed output where the interference noise caused by backscattering is reduced. (Frequency weighting normalization broadens the effective bandwidth and improves resolution). In our system, recombination of the signal ensemble is performed by a non linear minimization algorithm [1]. At each time instant this algorithm takes the minimum amplitude value $y_i(t)$ of the N filtered signals. Minimization is defined by :

$$y_i(t) = \min[|\chi(t,f_i)|] \qquad \text{for i=1, 2, …, N}$$

The randomness of the small scatterers giving uncorrelated data, only the coherent target pulses are retained. This algorithm is named absolute minimization and is highly sensitive to the localization of the analysis bandwidth (named B) in the echo spectrum. At time t, if no more target information is present in the analysis region, the corresponding frequency channels present a near zero amplitude and the algorithm misses the target even if a significant signal level is sensed in the remaining channels.

In the MBM process [3], we propose to slide the analysis bandwidth B between two limits fixed by the 20dB attenuation frequencies of the smoothed radio frequency (RF) spectrum. A set $y_i(t)$ of absolute minimizations starting from the low limit with a B analysis bandwidth and ?f increments are then performed to the upper limit.

The output $y(t)$ of the process is given by:

$$y(t)=\max[y_i(t)] \quad \text{with i=1,2,3…(N-B/?f)}$$

This algorithm selects signals presenting phase coherence characteristics over all frequency channels included in bandwidth B. (In the field of mathematical morphology B is called "structuring element"). As a result all specular echoes having a bandwidth equal to or larger then B are detected. This method becomes however questionable if we have to tackle frequency dependant absorbing materials which lead to variable B values.

In the next paragraph we try to illustrate how detection performance and structuring element B length are linked in the SSP time frequency representation.

<u>Time-frequency representation and structuring element selection :</u>
As an example consider a symmetrical echo, centered at $t=t_0$ and given by a sinusoid of frequency f_0 modulated by a gaussian envelope $g_0(t-t_0)$ (Fig 1a). This echo signal can be written:

$$x(t)=g_0(t-t_0).\cos(\omega_0(t-t_0))$$

If, as usually in SSP, the echo spectrum is processed by a gaussian filter bank $g(f-f_i)$ with center frequencies set at f_i, the time-frequency representation $\chi(t-f_i)$ can be expressed by :

$$\chi(t,f_i) = real\left[\sum_{i=1}^{N}(FT^{-1}(P(f)))\right],$$

$$\text{with } P(f) = \frac{1}{2}G(f-f_i)\left[G_0(f-f_0)+G_0(f+f_0)\right]e^{-2\pi.j.t_0} .$$

We notice that the bandwidth of the gaussian echo spectrum G_0 is always much larger than that of the windowing functions G_i. Thus we consider that the G_0 spectral amplitudes carved by each G_i window remain roughly constant and can be labeled α_i. The corresponding $\chi(t,f_i)$ time frequency representation is thus given by :

$$\chi(t,f_i) = \sum_{i=1}^{N}\alpha_i.g(t-t_0).\cos(2\pi f_i(t-t_0)) .$$

At time $t=t_0$ the echo amplitude and the cosine term are maximum. At this time $\chi(t,f_i)$ is maximum at each involved frequency, and the Split Spectrum method outputs a set of values α_i aligned along the frequency axis. This vertical alignment corresponds to the main lobe. The other maxima obey

$$2\pi f(t-t_0)=k\pi \text{ or } f = \frac{k}{2(t-t_0)} ,$$

and present a series of hyperbolic trajectories in the time-frequency plane (Fig.1b). It is easy to understand that the optimal structural element length B corresponds to bandwidth G_0. If B is set too large, then MBM will give no output at all and miss the echo. If B is chosen too small, MBM will provide several outputs and in actual experimental conditions lead to an increased probability of false detection (Fig.1d).
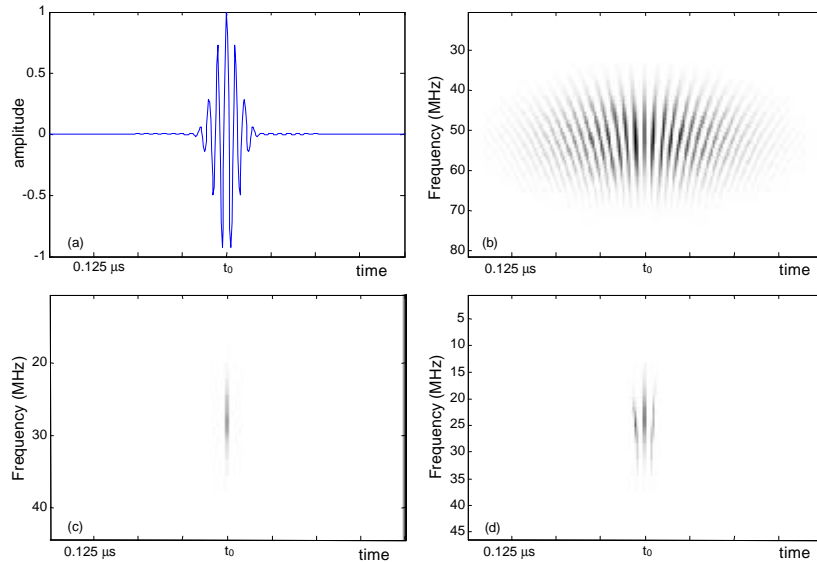

Figure 1
(a) : pulse echo   (b) : Time frequency representation
(c) : MBM detection with an optimal analysis bandwith
(d) : MBM detection with a too short analysis bandwith

3. THE VARIABLE MOVING BANDWITH MINIMIZATION

In figure 2 we show that in absorbing materials, the center frequency of the echo spectrum is shifted toward the lower frequencies and the spectral bandwidth shortens as a function of the observation depth. In order to take this bandwidth variation process into account, in the next paragraph we determine the spectral characteristics of the echo as a function of the observation depth.
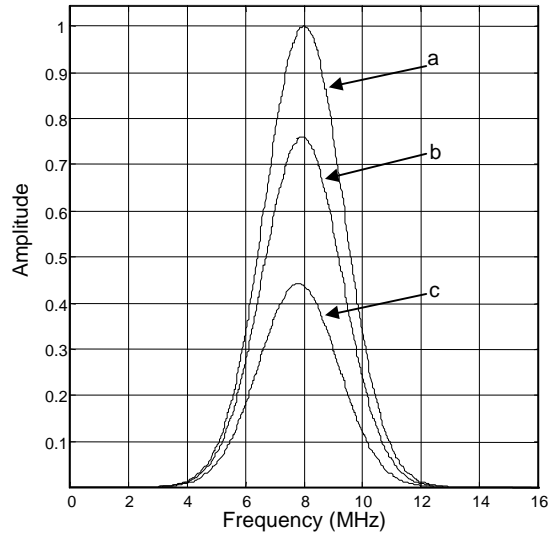

Figure 2

Examples of center frequency shift in a material having an attenuation of 3dB/MHz/mm :
(a) : original echo spectrum; (b) : spectrum of echo at 10μm; (c) : spectrum of echo at 30μm

Determination of the center frequency

The US field is focalized on a determined bubble located at a known depth. The corresponding RF echo is selected and Fourier transformed. The central frequency is obtained from a periodogram analysis [7]. The same operation is repeated for bubbles located at different depths. In figure 3 the central frequency is given as a function of bubble depth. We notice a quasi linear relation with depth varying from the surface to 600 μm.

Determination of the Bmin and Bmax spectral echo bandwidth

Ago we focalize on a reference bubble of known position. We start the test by choosing a large B value covering the whole echo spectrum. Beginning with this value we perform a first MBM calculation and observe the resulting time-frequency representation (TFR). The process is repeated until one vertical line, corresponding to the main lobe of the echo signal is imaged (see Fig. 1c). This last recorded B value is named Bmax.

The same process is performed with the difference that we start with the smallest possible B value (limit of frequency resolution). As long as lateral lobes are visible in the TFR B is incremented and a new MBM calculation performed. The process is stopped if the sole main lobe remains. The last entered B value is Bmin. The Bmin - Bmax couple is plotted in figure 3 as a function of inclusion depth.

From figure 4 we determine a linear relation giving the length of B as a function of the depth. In this way, B is always enclosed between the Bmin and Bmax limits. In the next part we describe the basic components of our ultrasound microscope system.
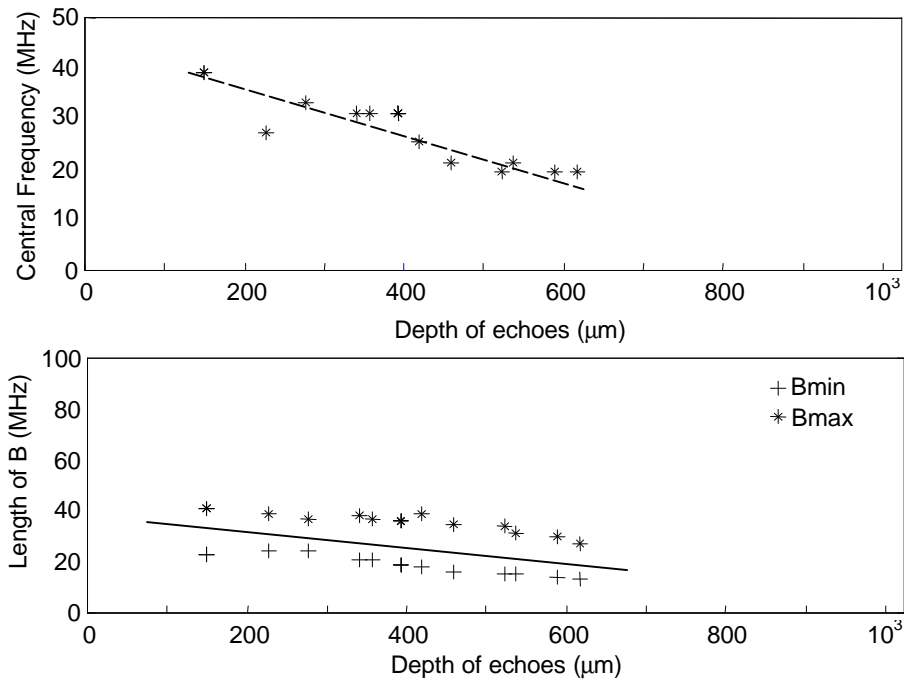
Figure 3
(a) Center frequency variation as a function of depth
(b) Minimum (Bmin) and maximum (Bmax) analysis bandwidth in function of depth

4. THE EXPERIMENTAL SET UP

Our acoustic microscope system is made of the following main elements :
- A Panametrics V390 SU/RM transducer of 6mm aperture, 12.5mm focal length, 120µm lateral resolution in water, and 44.5Mhz central frequency.
- A Panametrics 5627RPP pulse generator/receiver comprising an adjustable gain amplifier.
- A 54520A Hewlett Packard oscilloscope. The data are transferred to a personal computer via an IEEE488 link.
- The fixed transducer is automatically scanned in X and Y directions by a Microcontrole motion table driven by the computer.

Signal and image processing are performed with MATLAB ® 6.1.
In our epoxy polymer phantom the main US field propagation mode is longitudinal. The corresponding velocity depending on Young's modulus and Poisson's coefficient of the material was evaluated to 2480m/s (?=55.6µm).

We state that the adjustable physical parameters of our system have been set in a optimal manner. In the following we focalize particularly on our modified data processing method and show that this approach leads to improved performances of the ultrasound microscope.

5. US AND OPTICAL MICROSCOPE VIEWS COMPARISON

In a first step we compare three pictures of the same polymer area computed with MBM minimization using respectively ; B=24MHz, 30MHz, and a variable length structuring element (Fig. 5a, 5b and 5c).
On Fig 5a we observe a number of clouds of isolated pixels or blobs of a few pixels. Fig 5b presents a clean aspect; many bubbles detected with B=24MHz disappeared. The variable structuring element drawing (Fig. 5c) gives a representation that is close to the optical microscope image of figure 5d.
This picture is obtained with a Nikon SMZ-10 stereoscopic microscope equipped with a ×4 zoom. A visual comparison shows that the best fitting representation of the inclusions in our transparent epoxy polymer is provided by the variable structuring element minimization.
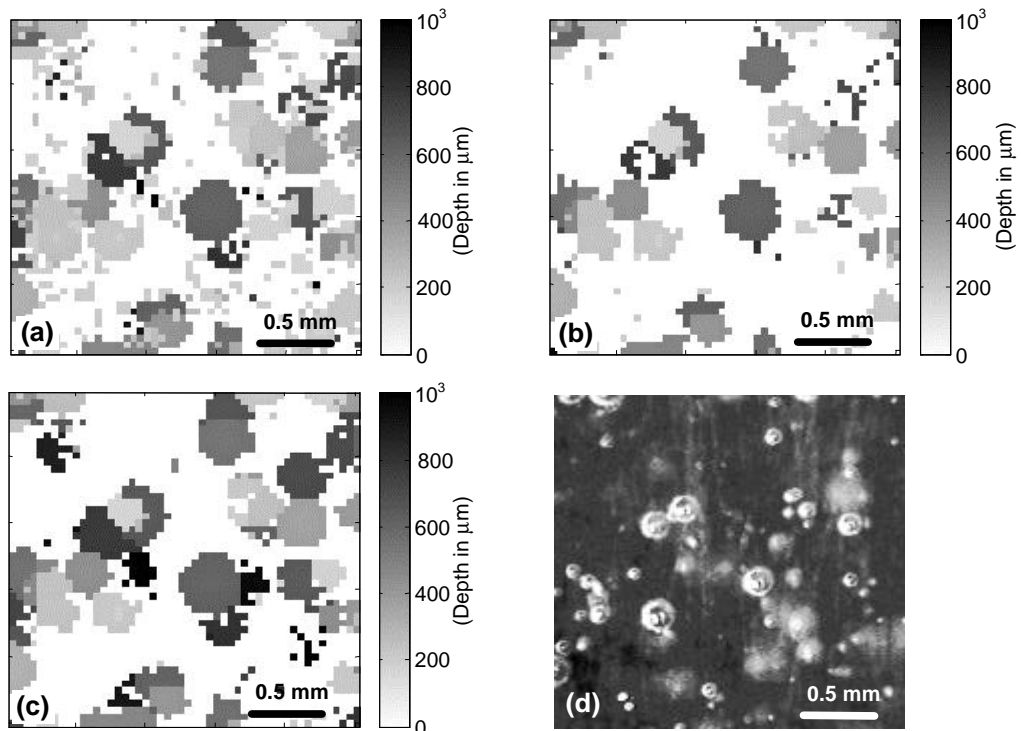
Figure 4

(a) depth image obtained with B=24 Mhz   (b) depth image with B=30 Mhz

(c) depth image obtained with variable B   (d) optical image of the polymer zone

6. CONCLUSION AND PERSPECTIVES

Comparing the ultrasound view with an optical image of the same polymer sample we can conclude that our ultrasound microscope provides representative images of the air bubble inclusions. On the other hand it appears that our variable structuring element minimization gives better results that the classical fixed bandwidth algorithms.

If we isolate an isolated bubble on both images and compare the diameters, we observe that the US picture provides systematically larger values. This broadening results from the convolution of the actual object with the limited spatial resolution of the US imaging system. A next investigation step will be to measure the spatial point spread function (PSF) of the system and to deconvolve the SSP minimization images. A further development will be to image an opaque noisy sample and to quantify accurately the inclusion rate in the polymer coating.

REFERENCES:

1) Karpur, P, Shankar, P.M., Rose, J.L., and Newhouse, V.L., Split Spectrum Processing : Optimizing the processing parameters using minimization, Ultrasonics, Vol 25, pp 204-208, 1987.
2) Tian, Q, and Bilgutay, N.H., Statistical analysis of Split Spectrum Processing, 1996 IEEE Ultrasonics Symposium, pp 709-712, 1996.
3) Karpur, P, Shankar, P.M., Rose, J.L., and Newhouse, V.L., Split Spectrum Processing : Determination of the available bandwidth for spectral splitting, Ultrasonics, Vol.26, pp 204-209, 1998
4) Grevillot, M, Cudel, C, Meyer, J.J., and Jacquey, S, Two approaches to multiple specular echo detection using Split Spectrum Processing : Moving bandwidth minimization and mathematical morphology, Ultrasonics, Vol 37, pp 417-422, 1999.
5) Grevillot M, Cudel C, Bacza F, Simonin L, Meyer J.J., Hunsinger J.J., Validation of a 3D ultrasound microscopy system designed for detection of air bubble inclusions in thermal spray polymer, Insight, Vol 42, pp 730-733, 2000.
6) Kuttruff, H, Ultrasonics Fundamentals and Applications, Elsevier Applied Science, 1991.
7) Oppenheim, A.V., and Schafer, R.W., Discrete-time signal processing, Prentice Hall, Signal Processing Series, pp 730-742, 1989.